Antikaon-nucleon/nuclei interactions at low-energy by AMADEUS

Raffaele Del Grande*

Istituto Nazionale di Fisica Nucleare
LABORATORI NAZIONALI DI FRASCATI

On the behalf of the AMADEUS collaboration

3rd Jagiellonian Symposium on Fundamental and Applied Subatomic Physics

Collegium Maius, Cracow, POLAND
June 23 - 28, 2019

UNIWERSYTET JAGIELLOŃSKI W KRAKOWIE

*raffaele.delgrande@lnf.infn.it

Motivation and Scientific Case

The investigation of the **in-medium modification of the $\bar{K}N$ interaction** is of fundamental importance for the understanding of low-energy QCD, in the so-called non perturbative regime.

Chiral perturbation theory (ChPT): effective field theory where mesons and baryons represent the effective degrees of freedom instead of the fundamental quark and gluon fields.

$$\mathcal{L}_{eff} = \mathcal{L}_{mesons}(\Phi) + \mathcal{L}_B(\Phi, \Psi_B)$$

- The chiral symmetry is **spontaneously broken**, implying the existence of massless and spinless Nambu-Goldstone bosons which are identified with the pions.
- It has proven to be **very successful** in describing the πN, $\pi\pi$ and NN interactions in the low-energy regime and is considered as the theory of the low-energy strong interaction **in the SU(2) flavour sector**.

The extension of the theory to the sector with the quark s turns out to be more problematic since it is not applicable to the $\bar{K}N$ channel.

Motivation and Scientific Case

The **ChPT is not applicable** to the $\bar{K}N$ channel due to the emerging of the $\Lambda(1405)$ and the $\Sigma(1385)$ resonances just below the $\bar{K}N$ mass threshold (~1432 MeV).

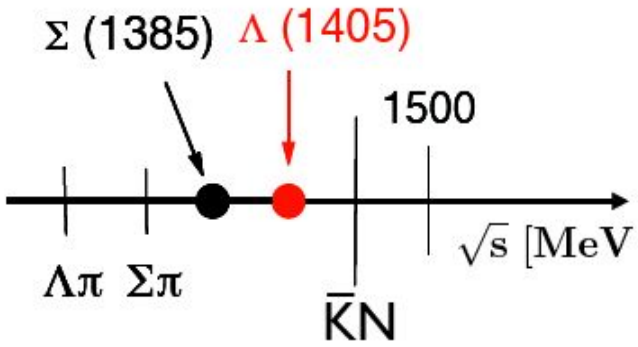

- $\Lambda(1405)$ I=0 $J^P = ½^-$
  M = $(1405.1^{+1.3}_{-1.0})$ MeV Γ = (50.5 ± 2.0) MeV
  decay modes: Σπ (I=0) 100%

- $\Sigma(1385)$ I=1 $JP = 3/2^+$

  decay modes: Λ π (I=1) (87.0 ± 1.5) %
  Σ π (I=1) (11.7 ± 1.5) %

Possible solutions:

➢ **Non-perturbative Coupled Channels approach: Chiral Unitary SU(3) Dynamics**

➢ **Phenomenological $\bar{K}N$ and NN potentials**

Motivation and Scientific Case

The parameters of the models are constrained by the existing K^-p elastic and inelastic scattering data from bubble chamber experiments above the $\bar{K}N$ threshold

Phen. [Y. Ikeda and T. Sato, Phys. Rev. C76, 035203 (2007)]
Chiral [S. Ohnishi, Y. Ikeda, T. Hyodo, W. Weise, Phys.Rev. C93 (2016) no.2, 025207]

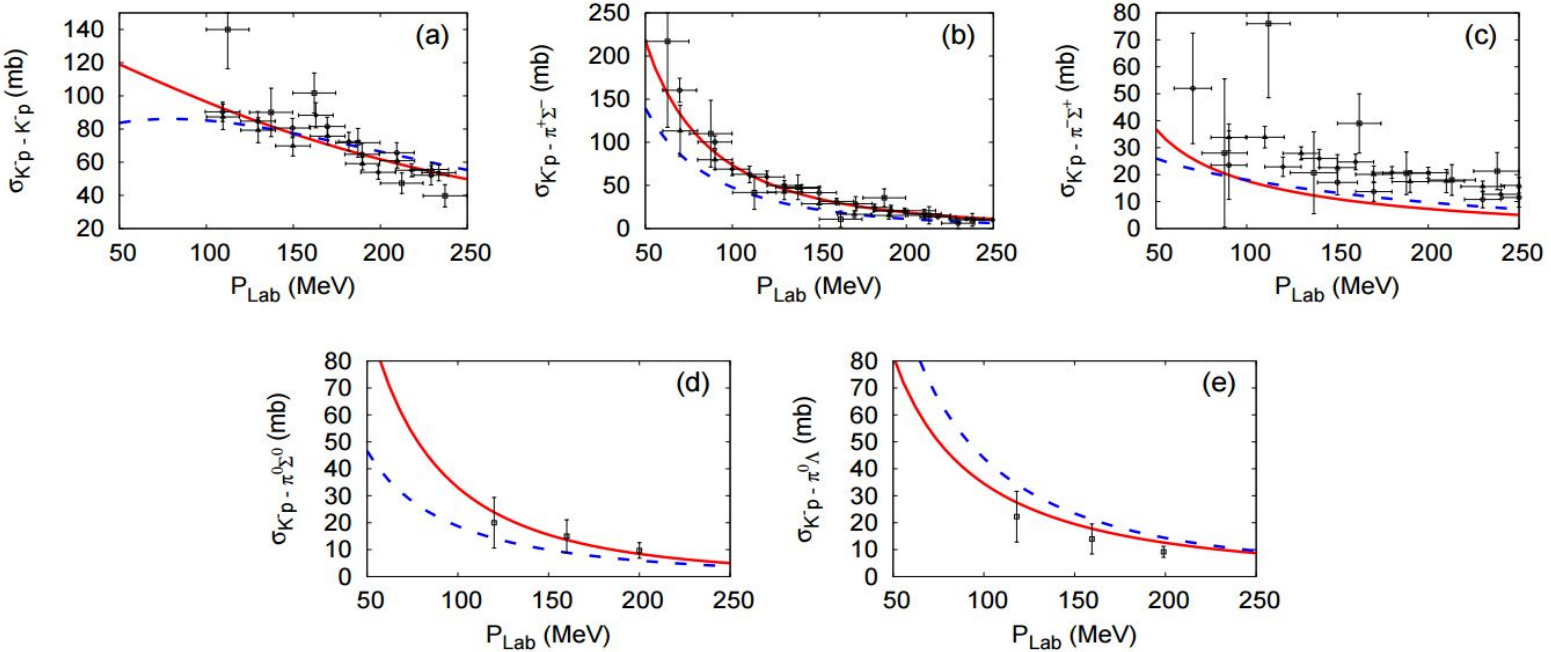

Motivation and Scientific Case

and by the precise SIDDHARTA measurement of K_α transition in Kaonic hydrogen at threshold

M. Bazzi et al.. 2011. (SIDDHARTA Coll.), Phys. Lett. B704, 113

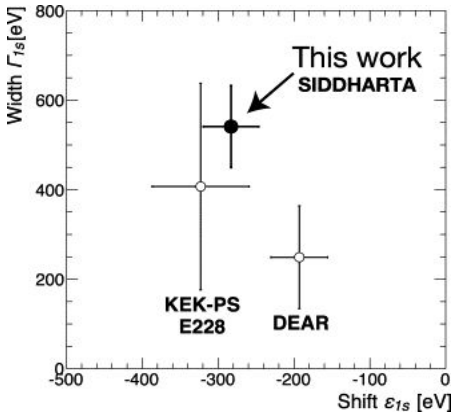

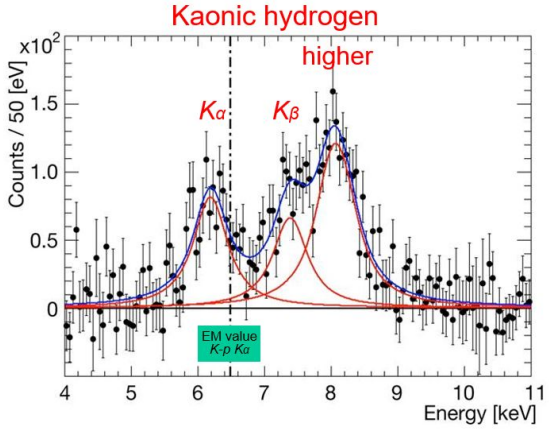

$$\varepsilon_{1S} = -283 \pm 36(\text{stat}) \pm 6(\text{syst}) \text{ eV}$$
$$\Gamma_{1S} = 541 \pm 89(\text{stat}) \pm 22(\text{syst}) \text{ eV}$$

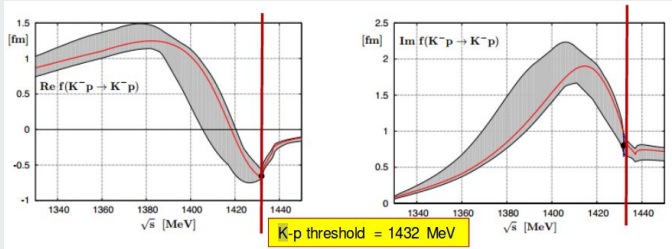

Fig. 3. Real part (left) and imaginary part (right) of the $K^-p \to K^-p$ forward scattering amplitude extrapolated to the subthreshold region. The empirical real and imaginary parts of the K^-p scattering length deduced from the recent kaonic hydrogen measurement (SIDDHARTA [7]) are indicated by the dots including statistical and systematic errors. The shaded uncertainty bands are explained in the text.

used to constraint the models at threshold

$$\varepsilon + \frac{i\Gamma}{2} = 2\alpha^3 \mu^2 a_{K^-p} = 412 \frac{eV}{fm} a_{K^-p}$$

Motivation and Scientific Case

Re Im

Phen. [Y. Akaishi, T. Yamazaki, Phys. Rev. C65, 044005 (2002)]
Chiral [Y. Ikeda, T. Hyodo, W. Weise, Phys. Lett. B706, 63 (2011)]

Phenomenological potential model

Chiral SU(3) dynamics

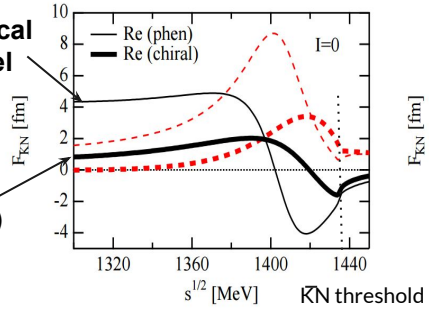

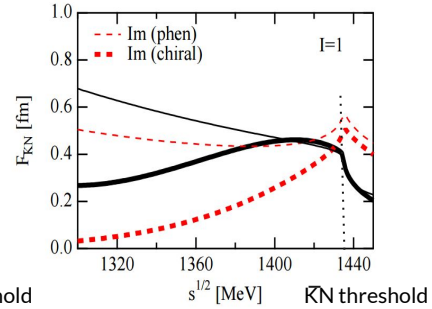

...but... discrepancies in the subthreshold extrapolations!

Significantly weaker attraction in chiral SU(3) models than in phenomenological potential models.

New experimental constraints are needed!!!

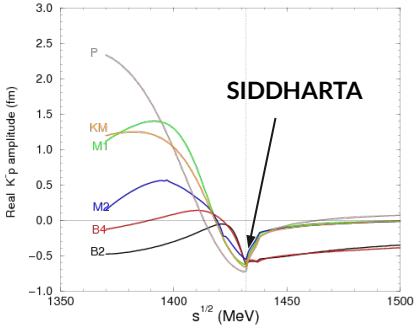

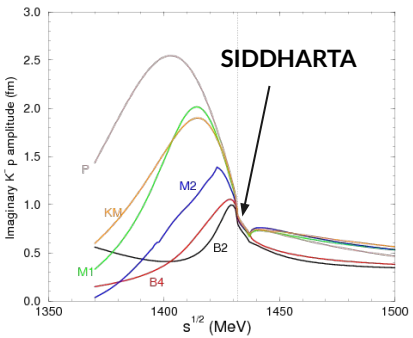

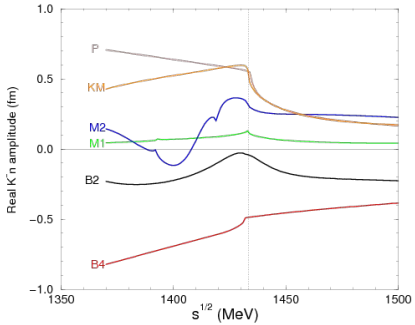

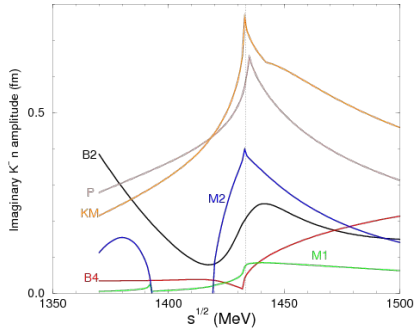

from E. Friedman, A. Gal, Nucl.Phys. A959 (2017) 66-82

The controversial nature of the Λ(1405)

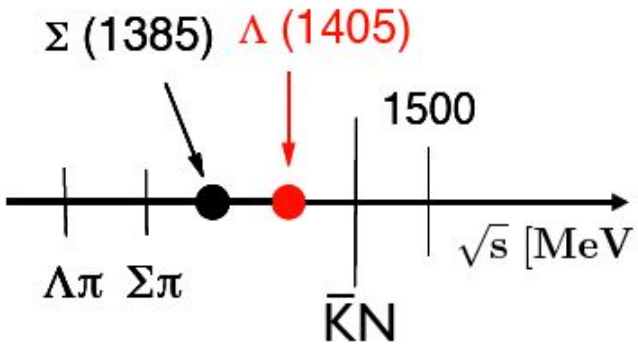

The Λ(1405) state does not fit with the simple three quarks model (*uds*) and it is commonly accepted that **it is, at least partially, a K̄N bound state**.

decay modes: Σπ (I=0) 100%

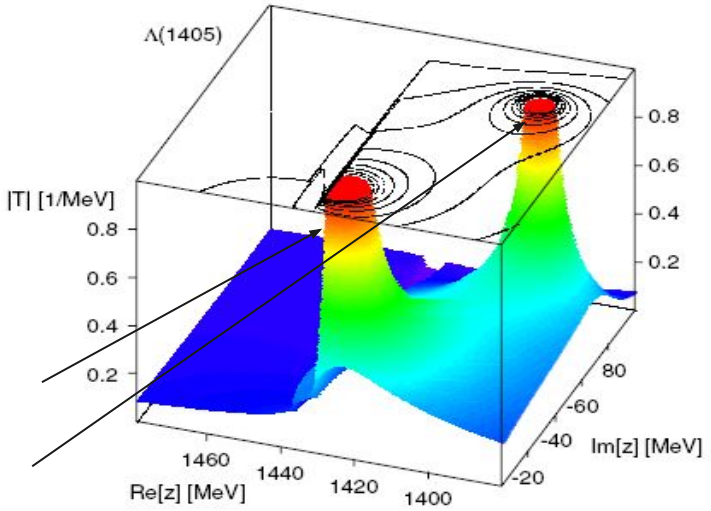

- **Chiral SU(3) coupled channel dynamics:**
  the state is given by the superpositions of **two poles of the K̄N scattering amplitude**.

  M = 1425 MeV → mainly coupled to the K̄N channel

  M = 1380 MeV → mainly coupled to the Σπ channel

The relative contributions of the two poles have to be measured experimentally

The controversial nature of the Λ(1405)

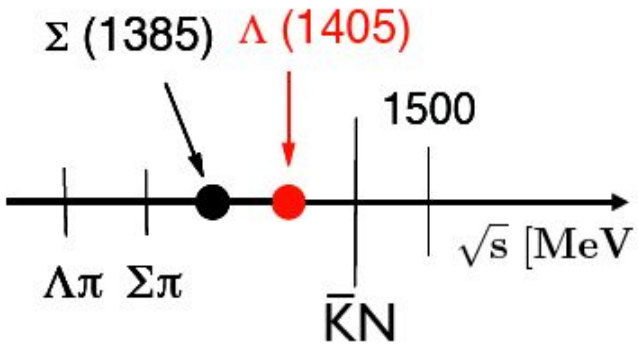

The Λ(1405) state does not fit with the simple three quarks model (*uds*) and it is commonly accepted that **it is, at least partially, a K̄N bound state**.

- **Esmaili-Akaishi-Yamazaki phenomenological potentials model:**
  according to the model by Esmaili-Akaishi-Yamazaki the **Λ(1405) is a pure K̄N bound state** with mass M=1405 MeV, binding energy BE = 27 MeV and width Γ=50 MeV.

  [Phys. Lett. B 686 (2010) 23-28]

  Single pole or two poles?

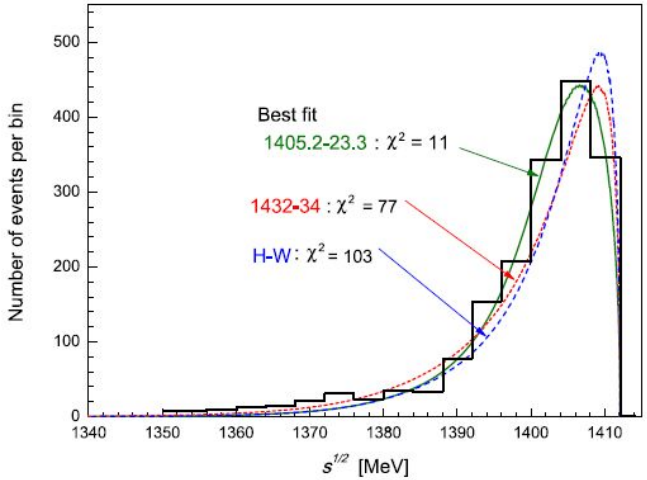

Fig. 6. Detailed differences in $M_{\Sigma\pi}$ spectra among the Hyodo–Weise prediction and the present model predictions.

The controversial nature of the Λ(1405)

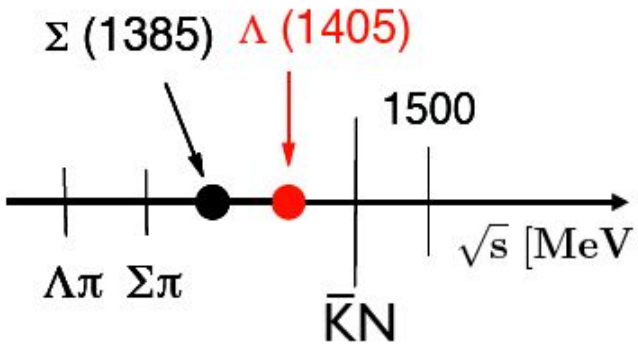

The Λ(1405) state does not fit with the simple three quarks model (*uds*) and it is commonly accepted that **it is, at least partially, a K̄N bound state**.

- **Esmaili-Akaishi-Yamazaki phenomenological potentials model:**
  according to the model by Esmaili-Akaishi-Yamazaki the **Λ(1405) is a pure K̄N bound state** with mass M=1405 MeV, binding energy BE = 27 MeV and width Γ=50 MeV.

  [Phys. Lett. B 686 (2010) 23-28]

  Single pole or two poles?

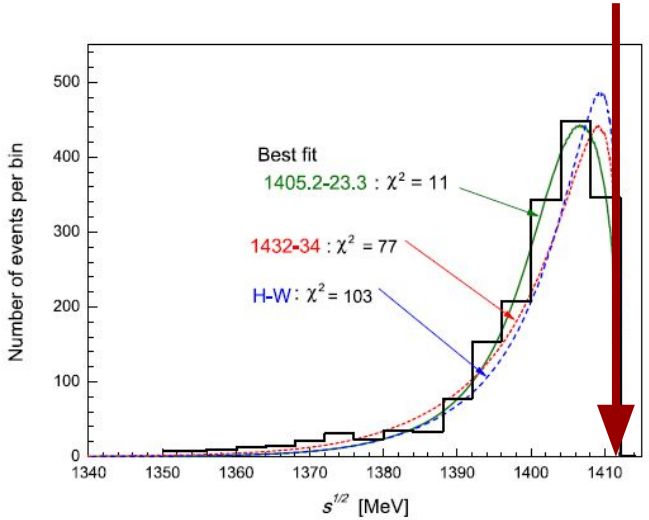

Fig. 6. Detailed differences in $M_{\Sigma\pi}$ spectra among the Hyodo–Weise prediction and the present model predictions.

Possible existence of kaonic bound state

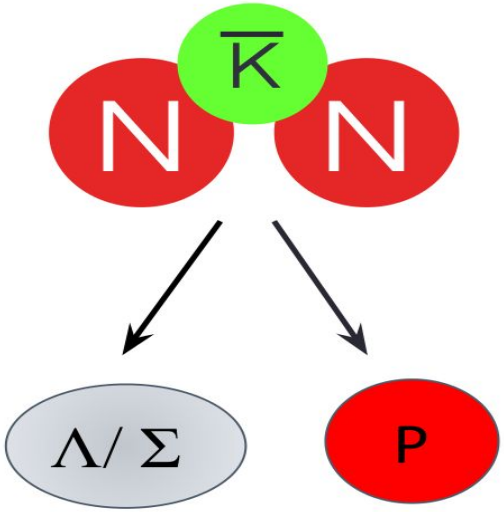

The fundamental kaonic bound state is the K^-pp cluster (and its isospin partner $\bar{K}^0pn$).

Main decay modes: $K^-pp \rightarrow \Lambda + p$
$\rightarrow \Sigma^0 + p$

○ **Chiral models**: Slightly bound states
BE ~ 10-30 MeV

▲ **Phen. approach**: Deeply bound states
BE ~ 40-100 MeV

Theory

	BE (MeV)	Γ (MeV)	Reference
○ Dote, Hyodo, Weise	17-23	40-70	Phys.Rev.C79 (2009) 014003
▲ Akaishi, Yamazaki	48	61	Phys.Rev.C65 (2002) 044005
○ Barnea, Gal, Liverts	16	41	Phys.Lett.B712 (2012) 132-137
▲ Ikeda, Sato	60-95	45-80	Phys.Rev.C76 (2007) 035203
○ Ikeda, Kamano, Sato	9-16	34-46	Prog.Theor.Phys. (2010) 124(3): 533
▲ Shevchenko, Gal, Mares	55-70	90-110	Phys.Rev.Lett.98 (2007) 082301
▲ Revai, Shevchenko	32	49	Phys.Rev.C90 (2014) no.3, 034004
▲ Maeda, Akaishi, Yamazaki	51.5	61	Proc.Jpn.Acad.B 89, (2013) 418
○ Bicudo	14.2-53	13.8-28.3	Phys.Rev.D76 (2007) 031502
○ Bayar, Oset	15-30	75-80	Nucl.Phys.A914 (2013) 349
▲ Wycech, Green	40-80	40-85	Phys.Rev.C79 (2009) 014001
○ Sekihara, Oset, Ramos	16	72	Prog.Theor.Phys. (2016) no.12, 123D03
○ Sekihara, Oset, Ramos	20	80	see E. Oset talk

Possible existence of kaonic bound state

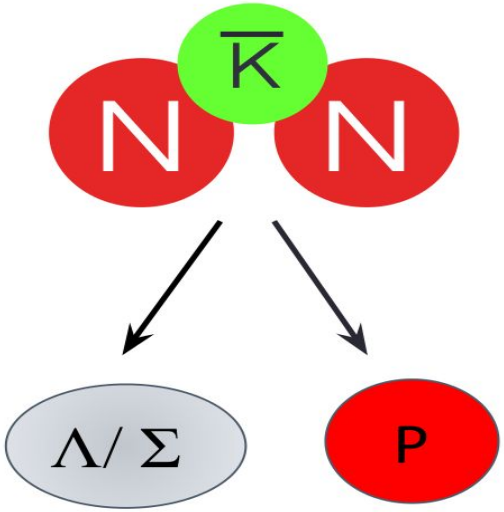

The fundamental kaonic bound state is the K^-pp cluster (and its isospin partner $\bar{K}^0pn$).

Main decay modes: $K^-pp \rightarrow \mathbf{\Lambda} + \mathbf{p}$
$\rightarrow \mathbf{\Sigma^0} + \mathbf{p}$

production mechanisms:

- p-p collisions
- K^- induced reactions
- π induced reactions
- photoproduction
- anti-p annihilations

Experiments

Experiment	BE (MeV)	Γ (MeV)	Reference
FINUDA	$115\ ^{+6}_{-5}$ (stat.) $^{+3}_{-4}$ (syst.)	$67\ ^{+14}_{-11}$ (stat.) $^{+2}_{-3}$ (syst.)	PRL 94 (2005), 212303
OBELIX	160.9 ± 4.9	$< 24.4 \pm 8.0$	NPA 789 (2007), 222
E549	-	-	MPLA 23 (2008), 2520
DISTO	103 ± 3 (stat.) ± 5 (syst.)	118 ± 8 (stat.) ± 10 (syst.)	PRL 104 (2010), 132502
LEPS/SPring-8	Upper Limit		PLB 728 (2014), 616
HADES	Upper Limit		PLB 742 (2015), 242
E27	$95\ ^{+18}_{-17}$ (stat.) $^{+30}_{-21}$ (syst.)	$162\ ^{+87}_{-45}$ (stat.) $^{+66}_{-78}$ (syst.)	PTEP (2015), 021D01
AMADEUS	Upper Limit		PLB 758 (2016), 134
E15	$15\ ^{+6}_{-8}$ (stat.) ± 12 (syst.)	$110\ ^{+19}_{-17}$ (stat.) ± 27 (syst.)	PTEP (2016), 051D01
E15 (2^{nd} run)	47 ±3 (stat.) $^{+3}_{-6}$(syst.)	115 ±7 (stat.) $^{+10}_{-20}$(syst.)	PLB 789 (2019), 620

Experimental search in K^- induced reactions

FINUDA at DAΦNE: $K^-_{stop} + X \rightarrow \Lambda + p + X'$

only back-to-back Λp pairs ($\cos\theta_{\Lambda p} < -0.8$)

detected particles

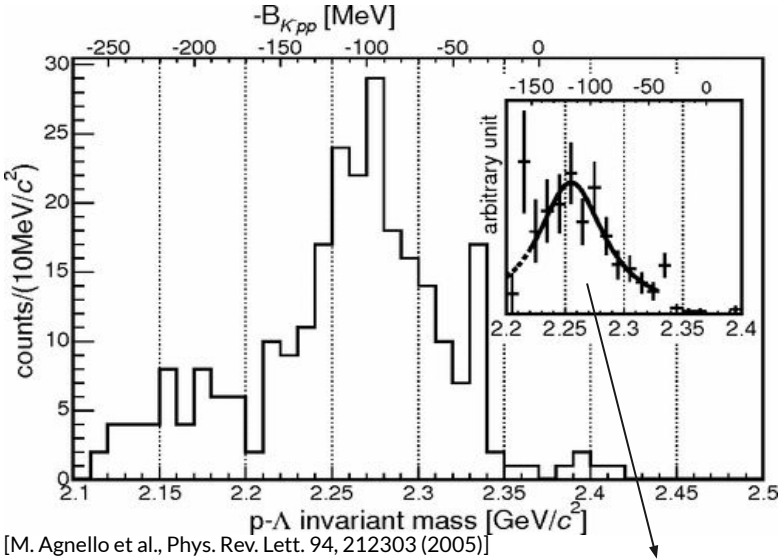

[M. Agnello et al., Phys. Rev. Lett. 94, 212303 (2005)]

Interpreted as the signal of:

$K^-pp \rightarrow \Lambda + p$

extracted parameters:

BE = $(115^{+6}_{-5}\,(stat.)^{+3}_{-4}\,(syst.))$ MeV

Γ = $(67^{+14}_{-11}(stat.)^{+2}_{-3}(syst.))$ MeV/c^2

E549 at KEK: $K^-_{stop} + {}^4He \rightarrow \Lambda + p + X'$

detected particles

[T. Suzuki et al., Mod. Phys. Lett. A23 (2008) 2520-2523.]

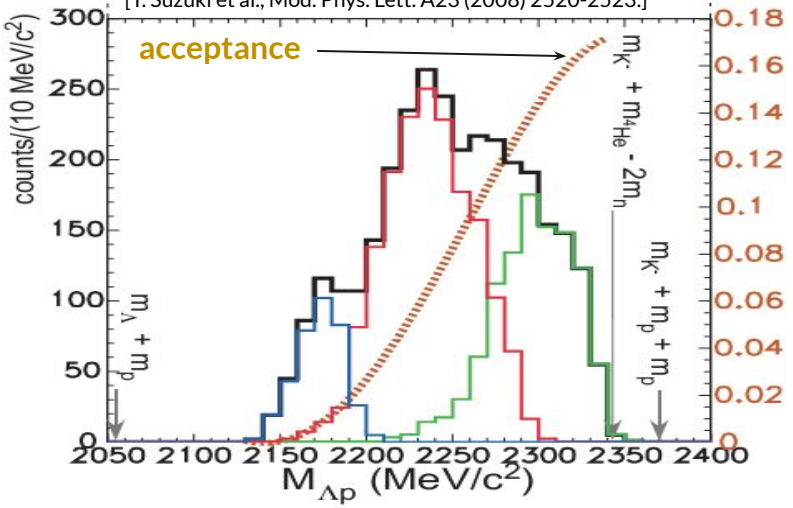

Using the missing mass information, three components to the invariant mass spectrum are found:

- **1NA**: K^- single nucleon absorption
- **2NA**: K^- two nucleon absorption
- **2NA + conversion**, **multi-nucleon**, **or Bound State**?

K^- multi-nucleon absorptions

In K^--nuclei optical potential a K^- multi-nucleon absorption term is necessary to fit the kaonic atoms data:

$$V_{K^-}(\rho) = V_{K^-}^{(1)}(\rho) + V_{K^-}^{(2)}(\rho)$$

→ **multi-nucleon term**

[E. Friedman, A. Gal, Nucl. Phys. A 959, 66 (2017)]
[Hrtánková, J. & Mareš, J. Phys. Rev. C96, 015205 (2017)]

single nucleon term from chiral models

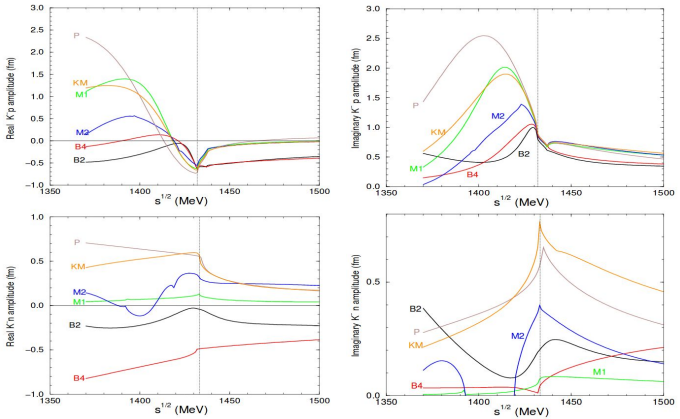

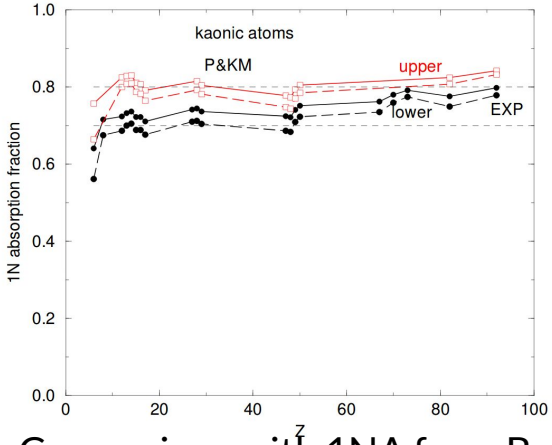

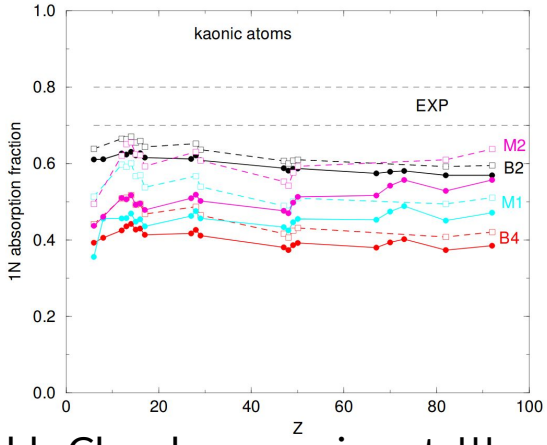

Comparison with 1NA from Bubble Chamber experiments!!!

Single and multi-nucleon K^- absorptions

- **Single nucleon absorption (1NA):** K^- "N" $\rightarrow Y\,\pi$ ⟶ pionic processes
- **Two nucleon absorption (2NA):** K^- "NN" $\rightarrow Y\,N$
- **Three nucleon absorption (3NA):** K^- "NNN" $\rightarrow Y\,(NN)$ ⟶ non-pionic processes
- **Four nucleon absorption (4NA):** K^- "NNNN" $\rightarrow Y\,(NNN)$

bound nucleons = "N", "NN", "NNN", "NNNN"
bound or unbound nucleons = (NN), (NNN)
Y = Λ, Σ

[Katz et al., Physical Review D (1970), Vol.1, No.5]

TABLE V. Comparative data on the frequency of emission of various particles.

	Hydrogen	Deuterium	Capture nucleus Helium (this experiment)	Helium (Helium Bubble Chamber Collaboration)[a]	(76% CF_3Br) + (24% C_3H_8)	Nuclear emulsion
$[\pi^\pm]/[K^-]$	0.64	0.67	0.55±0.05	0.55	0.45	0.40
$[\pi^-]/[\pi^+]$	0.46	1.95	4.9 ±1.0	5.5	3.8	3.9
$[\Sigma^\pm]/[K^-]$	0.64	0.46	0.31±0.03	0.27	0.19	0.187
$[\Sigma^+]/[\Sigma^-]$	0.46	0.73	1.2 ±0.2	1.16	1.05	0.79
$[\Sigma^+ + \pi^-]/[\Sigma^- + \pi^+]$	0.46	0.85	1.8 ±0.5	1.82	1.52	1.43
Multinucleon (i.e., nonpionic) capture	···	0.01	0.16±0.03	0.17±0.04[b]	0.25	0.15–0.30

[a] Reference 2.
[b] Nonpionic ratio of (32±2)% for K^- in He^4 was quoted by M. M. Block, in *Proceedings of the International Conference on Hypernuclear Physics, Argonne National Laboratory, Argonne, 1969*, edited by A. R. Bodmer and L. G. Hyman (ANL, Argonne, 1969).

CONTRIBUTIONS OF THE SEPARATE 2NA, 3NA and 4NA NEVER MEASURED!!!

Goals of AMADEUS

AMADEUS : **A**ntikaonic **M**atter **A**t **D**AΦNE: an **E**xperiment with **U**nraveling **S**pectroscopy

Unprecedented studies of the **low-energy charged kaons interactions in nuclear matter**: solid and gaseous targets (H, ^{4}He, ^{8}Be, ^{12}C ...) in order to obtain unique quality information about:

1. Controversial **nature of the Λ(1405)** and **K̄N amplitude below threshold**

2. **Low-energy** charged kaon **cross sections** for momenta of 100 MeV/c

3. a) Interaction of K^- with one and more nucleons (**single and multi–nucleon K^- absorption**)

   b) possible existence of **kaonic bound states**

4. **YN scattering** → extremely **poor experimental information** from scattering data (helpful to understand the EoS of Neutron Stars)

Yπ CORRELATION STUDIES
(i.e. Λπ and Σπ and final states)

YN CORRELATION STUDIES
(i.e. Λ p, Σ^0 p, and Λ t final states)

DAΦNE & AMADEUS

DAΦNE

- double ring $e^+ e^-$ collider working at C.M. energy of φ,
- producing **≈ 1000 φ /s**

$\varphi \rightarrow K^+ K^-$ (BR = (49.2 ± 0.6)%)

- **low momentum** Kaons ≈ 127 Mev/c
- **back to back** $K^+ K^-$ topology

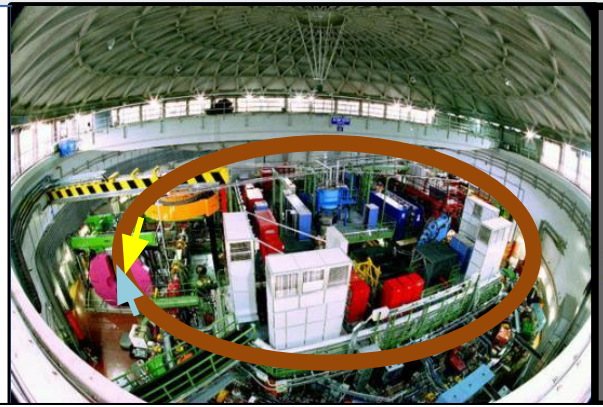

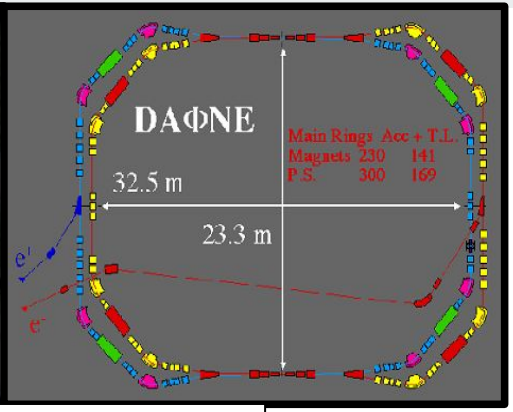

AMADEUS step 0 → KLOE 2004-2005 dataset analysis ($\mathcal{L}$ = 1.74 pb^{-1})

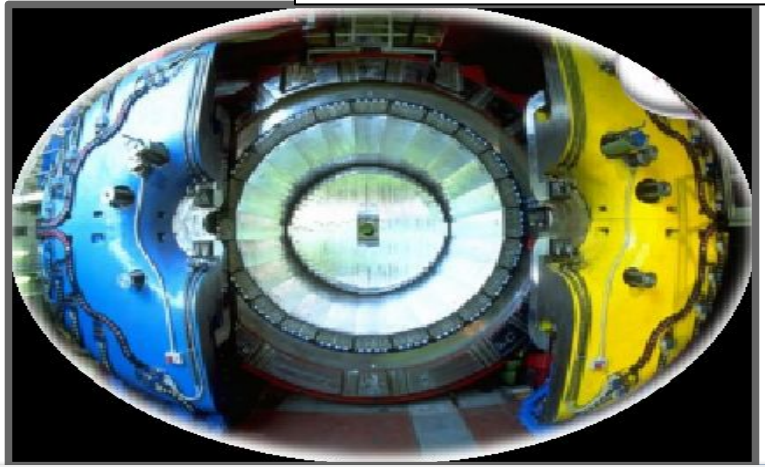

KLOE

- Cylindrical drift chamber with a **4π geometry** and electromagnetic calorimeter
- **96% acceptance**
- optimized in the energy range of all **charged particles** involved
- **good performance** in detecting **photons and neutrons** checked by kloNe group

[M. Anelli et al., Nucl Inst. Meth. A 581, 368 (2007)]

K^- absorption on light nuclei

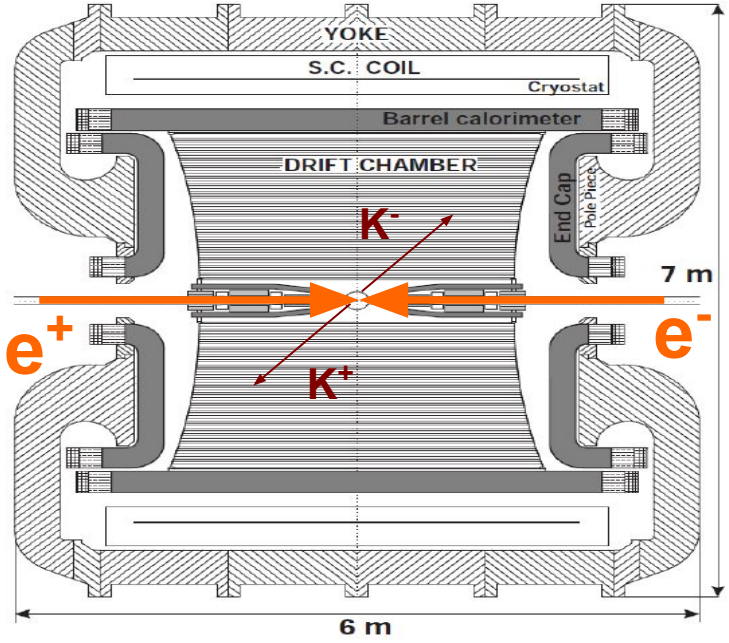

Possibility to use KLOE materials as an active target

- DC wall (750 μm C foil , 150 μm Al foil);
- DC gas (90% He, 10% C_4H_{10}).

Advantages:

Excellent resolutions..

$\sigma_{p\Lambda}$ = 0.49±0.01 MeV/c in DC gas

$\sigma_{m\gamma\gamma}$ = 18.3±0.6 MeV/c^2

Disadvantages:

Not dedicated target → different nuclei contamination → complex interpretation.

K^- absorptions at-rest and in-flight

Analyzed data: → KLOE 2004-2005 datataking (integrated luminosity: $\mathcal{L}$ = 1.74 fb^{-1})
→ 50% of K^- absorptions at-rest and 50% of K^- absorptions in-flight

AT-REST

K^- absorbed from atomic orbitals
(p_K ~ 0 MeV/c)

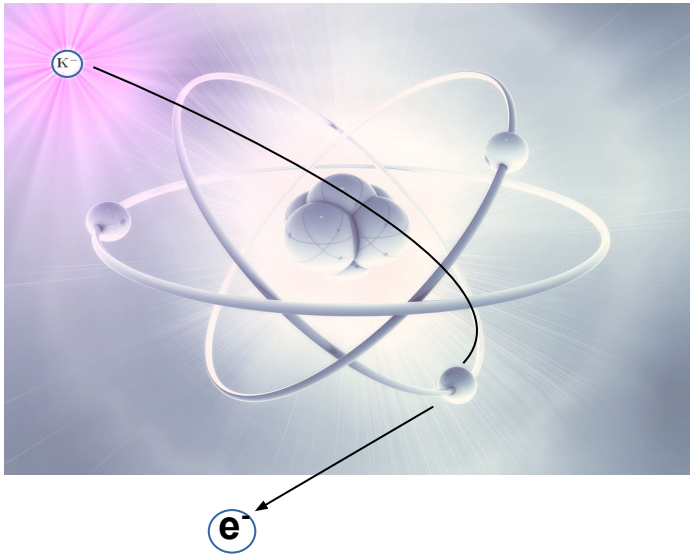

IN-FLIGHT

(p_K~ 100 MeV/c)

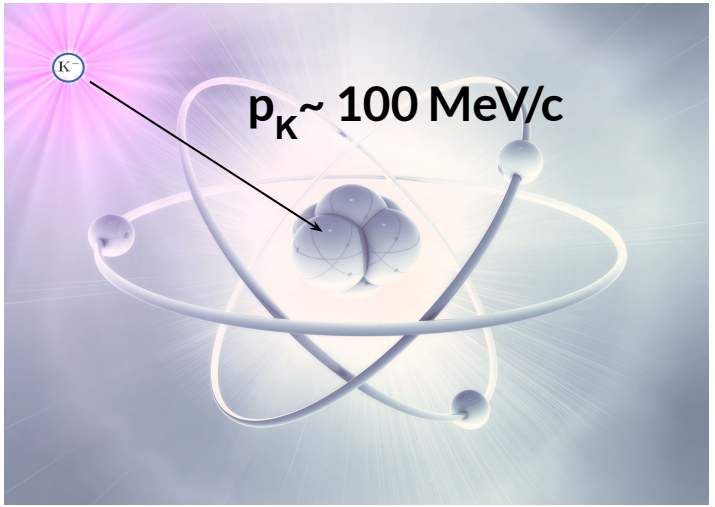

First determination of the non-resonant transition amplitude below threshold

Investigated using:

$K^- \text{“n”} \rightarrow \Lambda\pi^-$ to extract $|f^{N\text{-}R}_{\Lambda\pi}(I=1)|$

below threshold

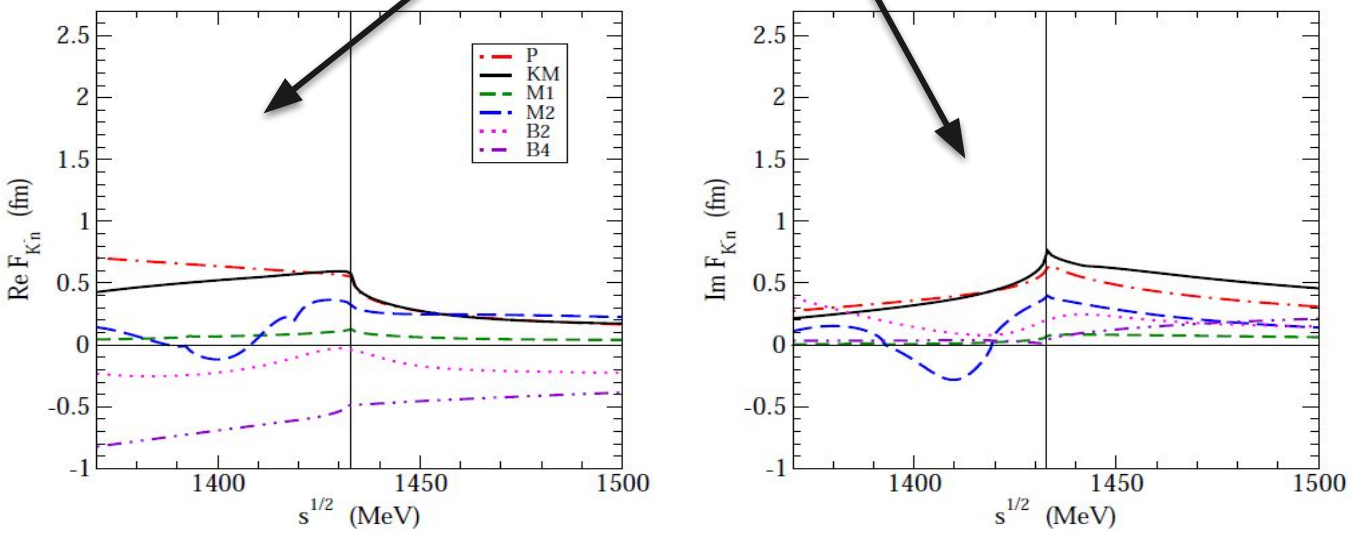

[J. Hrtankova, and J. Mares, Phys. Rev. C96, (2017) 015205]
[A. Cieply et al., Nucl. Phys. A954, (2016) 17]

Simultaneous fit : ($p_{\Lambda\pi^-}$ - $m_{\Lambda\pi^-}$ - $\cos(\theta_{\Lambda\pi^-})$

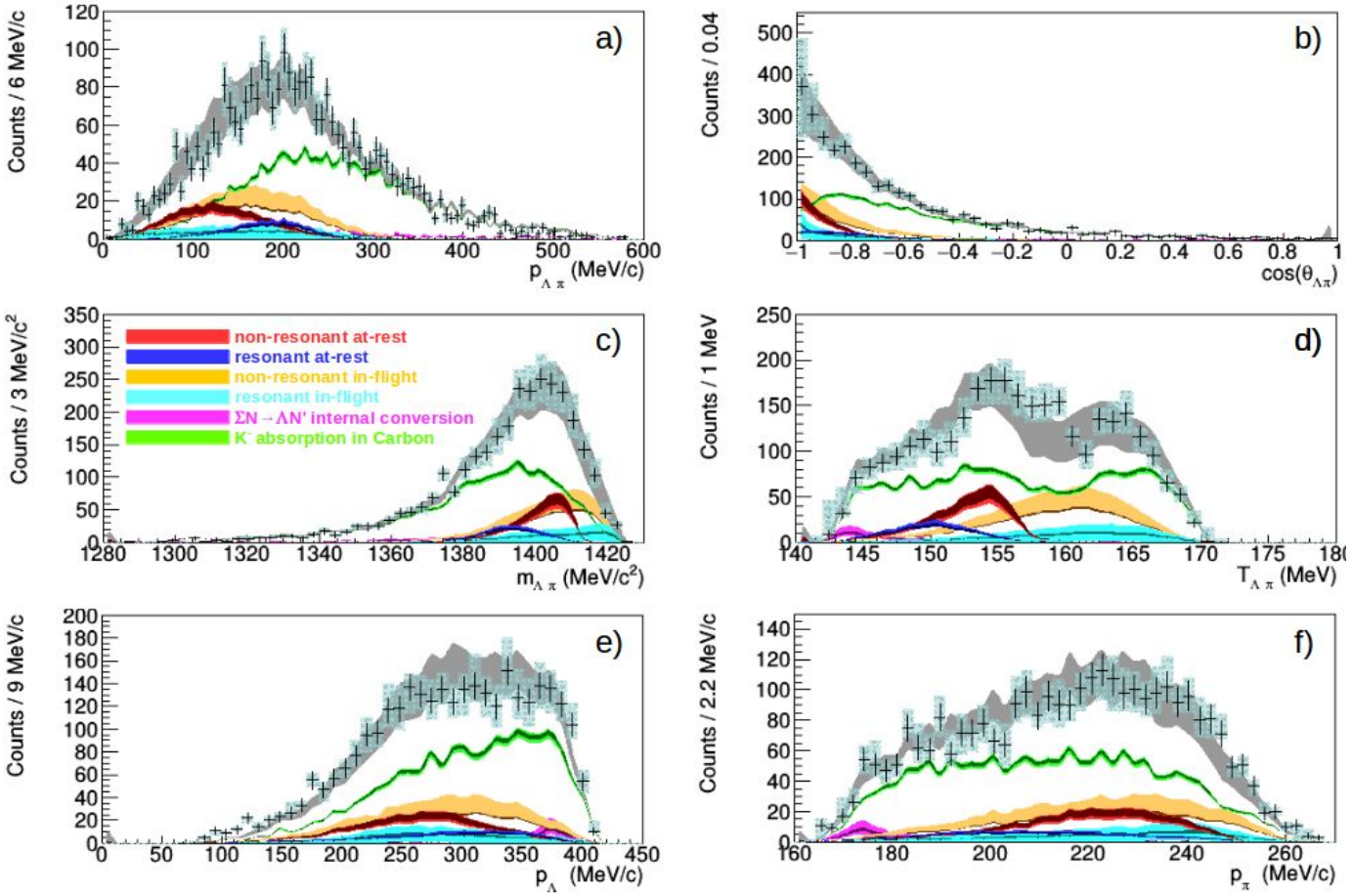

Simultaneous fit : ($p_{\Lambda\pi^-}$ - $m_{\Lambda\pi^-}$ - $\cos(\theta_{\Lambda\pi^-})$

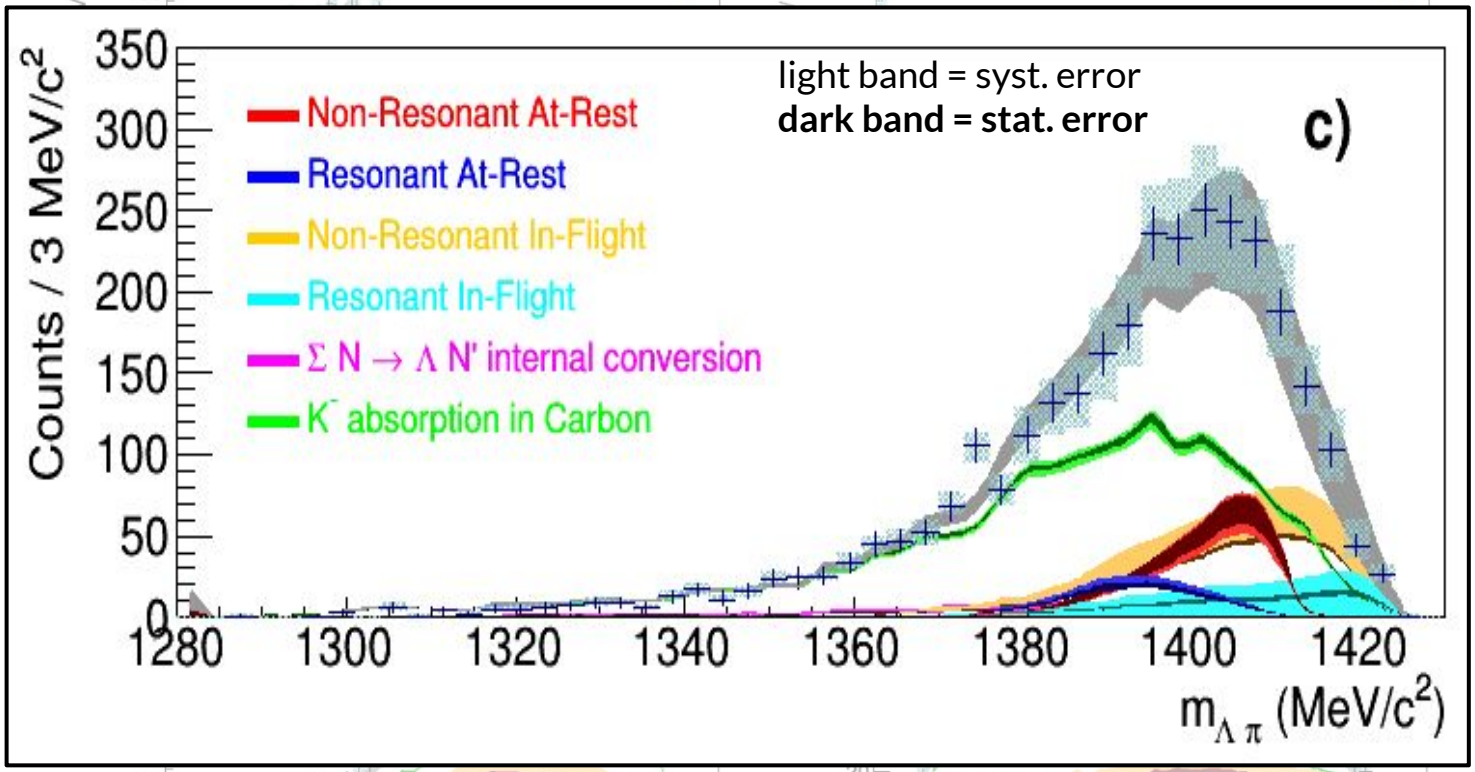

Outcome of the measurement

$$|f_{ar}^{s}| = (0.334 \pm 0.018\,\mathrm{stat}^{+0.034}_{-0.058}\mathrm{syst})\ \mathrm{fm}\,.$$

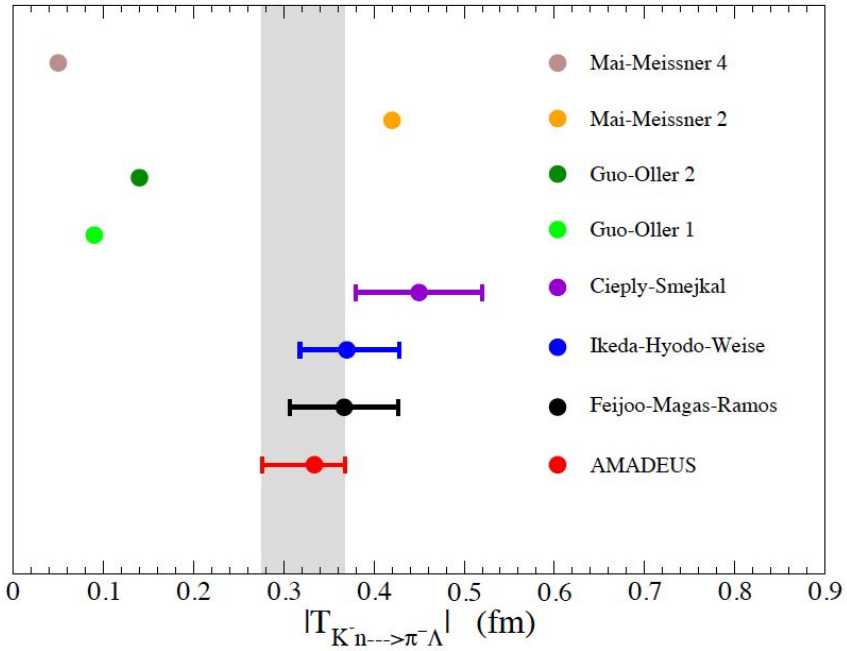

A. Feijoo, Volodymyr Magas, Angels Ramos, Phys.Rev. C99 (2019) no.3, 035211

K. Piscicchia, S. Wycech, L. Fabbietti et al. Phys.Lett. B782 (2018) 339-345

$A_{K\text{-}n \to \Lambda\pi^-}$ ($s^{1/2} \sim 1400$ MeV^{½})

$$E_{Kn} = -|B_n| - \frac{p_3^2}{2\mu_{\pi,\Lambda,^3He}}$$

[Nucl. Phys. A954 (2016) 75-93]

[Phys. Rev. C 96 (2017) 045204]

[Phys. Lett. B 702 (2011) 402–407]

[Nucl.Phys. A968 (2017) 35-47]

$K^- p \rightarrow \Sigma^0 \pi^0$ cross section

- cross section measurement at or below 100 MeV/c missing
- existing data at (120, 160, ..) MeV/c with big relative errors (about 50% at 120 MeV/c)

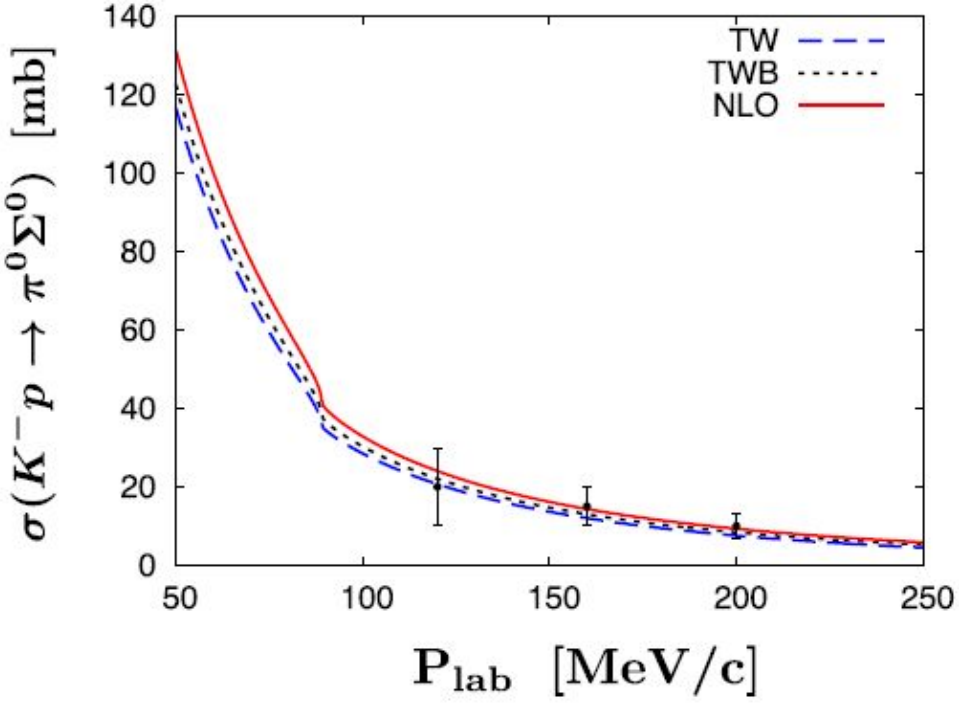

[Nuclear Physics A 881 (2012) 98–114]

$K^- p \rightarrow \Sigma^0 \pi^0$ cross section

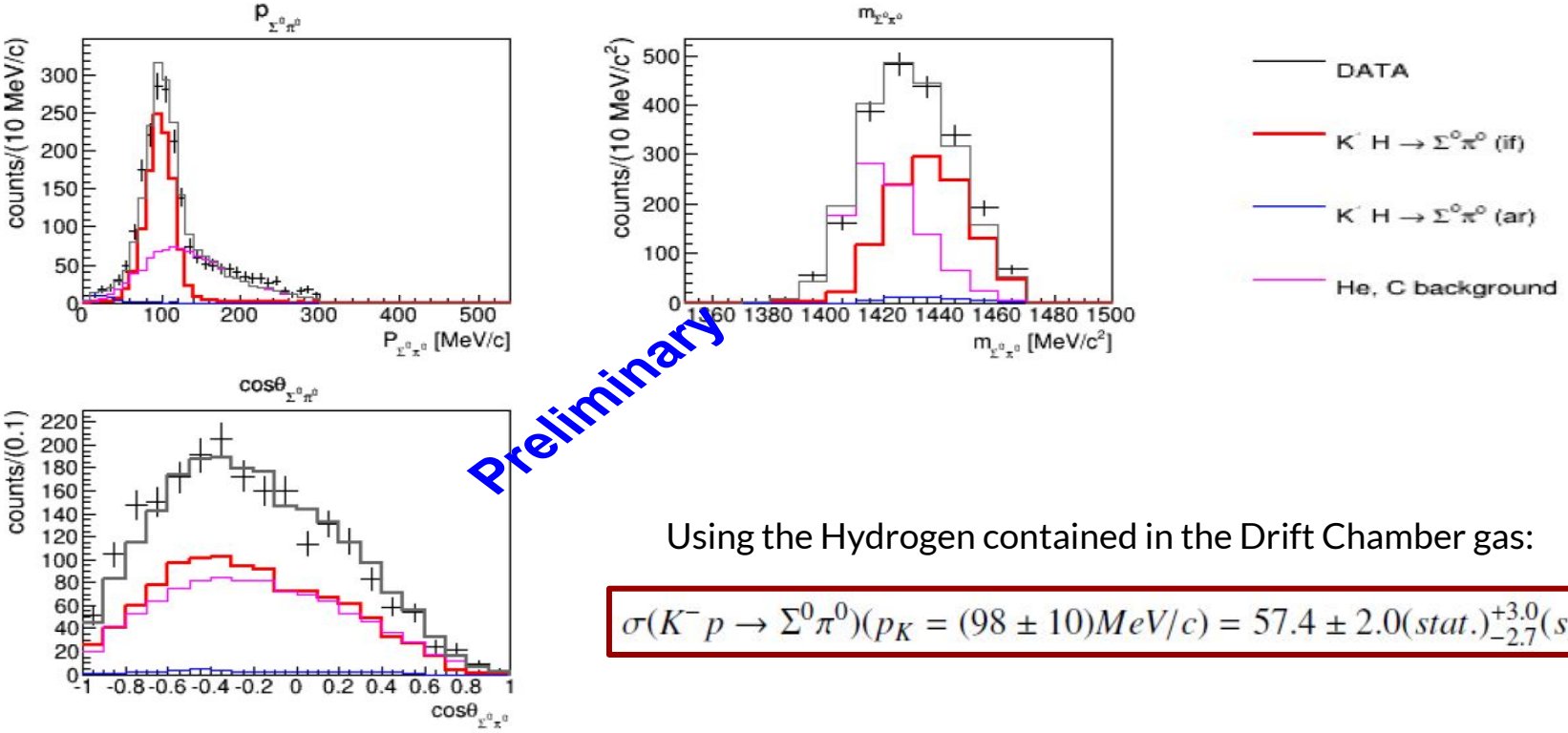

Using the Hydrogen contained in the Drift Chamber gas:

$$\sigma(K^- p \rightarrow \Sigma^0\pi^0)(p_K = (98 \pm 10) MeV/c) = 57.4 \pm 2.0(stat.)^{+3.0}_{-2.7}(syst.)\ \text{mb}$$

Figure 13. The simultaneous fit of $p_{\Sigma^0\pi^0}$ (left upper), $m_{\Sigma^0\pi^0}$ (right upper) and $cos\theta_{\Sigma^0\pi^0}$ (left lower). Black points represent the data, error bars correspond to the statistical errors, the gray line distributions represent the global fitting function. The colour legend for the different contributing processes is shown in the bottom right panel.

$K^-p \rightarrow \Sigma^0\pi^0$ cross section

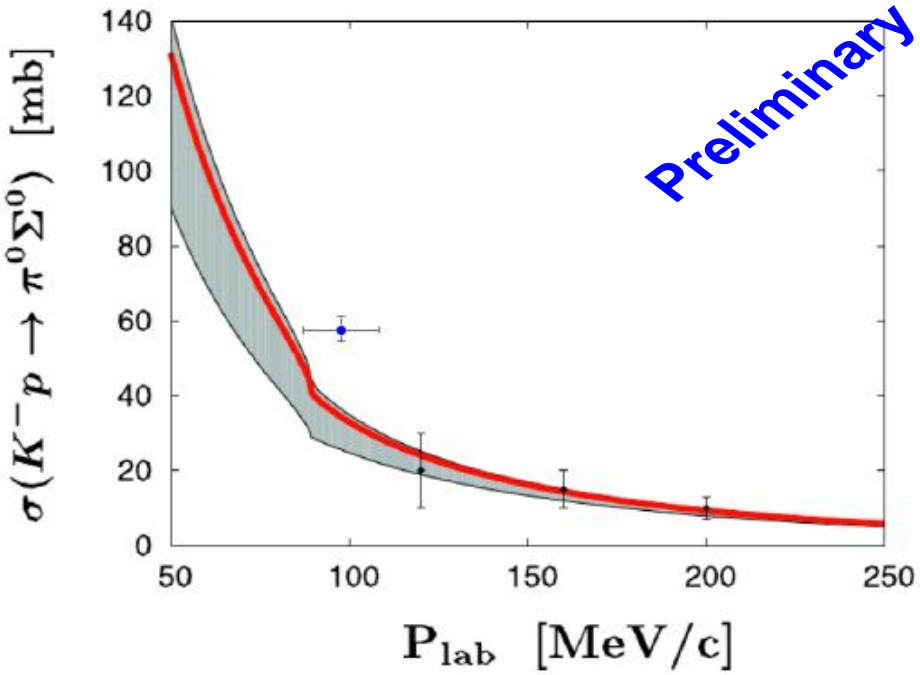

$$\sigma(K^- p \rightarrow \Sigma^0\pi^0)(p_K = (98 \pm 10) MeV/c) = 57.4 \pm 2.0(stat.)^{+3.0}_{-2.7}(syst.)\ \text{mb}$$

Figure 14. *$K^-p \rightarrow \Sigma^0\pi^0$ cross section as function of K^- laboratory momentum. The black points represent the experimental data from [15, 16], the corresponding uncertainty on the kaon momentum is not shown in this figure. The solid red curve with the shaded uncertainty band represents the theoretical calculation in Ref. [12]. The blue point is the measurement of this work.*

[15] W. E. Humphrey and R. R. Ross, Phys. Rev. 127 (1962) 1305
[16] J. K. Kim, Columbia University Report No. NEVIS-149 (1966)
[12] Y. Ikeda, T. Hyodo, W. Weise, Nucl. Phys. A 881 (2012) 98

Λp analysis: K^- multi-nucleon absorption BRs and σ

Simultaneous fit of:

- Λp invariant mass;
- angular correlation;
- proton momentum;
- Λ momentum.

Total reduced χ^2: χ^2/dof = 0.94

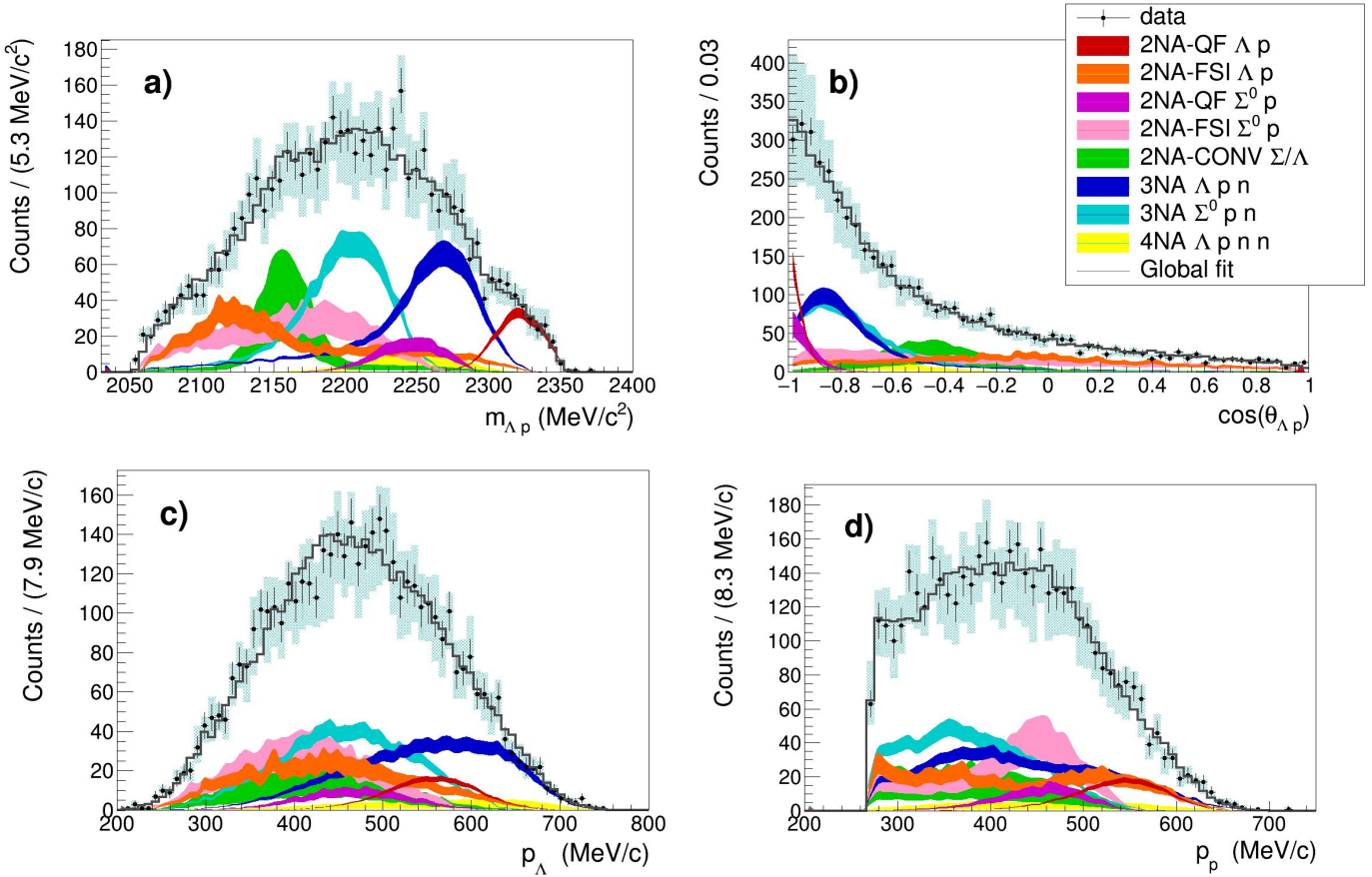

R. Del Grande, K. Piscicchia, O. Vazquez Doce et al., Eur.Phys.J. C79 (2019) no.3, 190

Λp analysis: K^- multi-nucleon absorption BRs and σ

	from stopped K^-	from in-flight K^-		
Process	Branching Ratio (%)	σ (mb)	@	p_K (MeV/c)
2NA-QF Λp	0.25 ± 0.02 (stat.) $^{+0.01}_{-0.02}$(syst.)	2.8 ± 0.3 (stat.) $^{+0.1}_{-0.2}$ (syst.)	@	128 ± 29
2NA-FSI Λp	6.2 ± 1.4(stat.) $^{+0.5}_{-0.6}$(syst.)	69 ± 15 (stat.) ± 6 (syst.)	@	128 ± 29
2NA-QF Σ^0p	0.35 ± 0.09(stat.) $^{+0.13}_{-0.06}$(syst.)	3.9 ± 1.0 (stat.) $^{+1.4}_{-0.7}$ (syst.)	@	128 ± 29
2NA-FSI Σ^0p	7.2 ± 2.2(stat.) $^{+4.2}_{-5.4}$(syst.)	80 ± 25 (stat.) $^{+46}_{-60}$ (syst.)	@	128 ± 29
2NA-CONV Σ/Λ	2.1 ± 1.2(stat.) $^{+0.9}_{-0.5}$(syst.)	-		
3NA Λpn	1.4 ± 0.2(stat.) $^{+0.1}_{-0.2}$(syst.)	15 ± 2 (stat.) ± 2 (syst.)	@	117 ± 23
3NA Σ^0pn	3.7 ± 0.4(stat.) $^{+0.2}_{-0.4}$(syst.)	41 ± 4 (stat.) $^{+2}_{-5}$ (syst.)	@	117 ± 23
4NA Λpnn	0.13 ± 0.09(stat.) $^{+0.08}_{-0.07}$(syst.)	-		
Global $\Lambda(\Sigma^0)$p	21 ± 3(stat.) $^{+5}_{-6}$(syst.)	-		

The ratio between the branching ratios of the 2NA-QF in the Λp channel and in the Σ^0p is measured to be:

$$\mathcal{R} = \frac{BR(K^- pp \to \Lambda p)}{BR(K^- pp \to \Sigma^0 p)} = 0.7 \pm 0.2(stat.)^{+0.2}_{-0.3}(syst.)$$

and the ratio between the corresponding phase spaces is $\mathcal{R}' \simeq 1.22$.

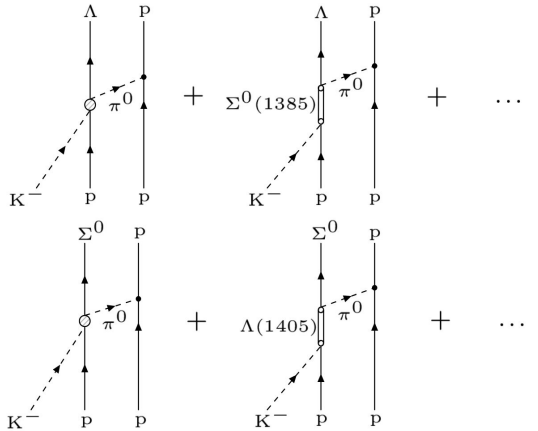

information on the in-medium properties of the Λ(1405).

R. Del Grande, K. Piscicchia, O. Vazquez Doce et al., Eur.Phys.J. C79 (2019) no.3, 190

Λp analysis: K⁻ pp bound state search

R. Del Grande, K. Piscicchia, O. Vazquez Doce et al., Eur.Phys.J. C79 (2019) no.3, 190

AMADEUS at DAΦNE

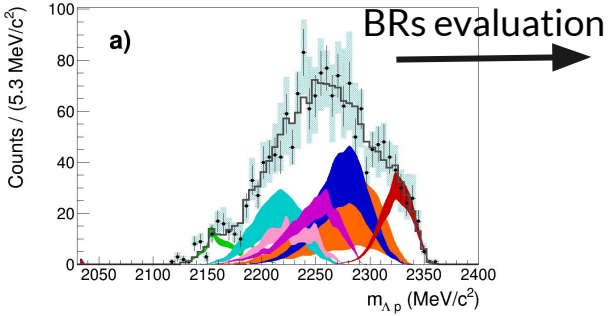

BRs evaluation

Process	Branching Ratio (%)
2NA-QF Λp	$0.20 \pm 0.04(\text{stat.}) \pm 0.02(\text{syst.})$
2NA-FSI Λp	$3.8 \pm 2.3(\text{stat.}) \pm 1.1(\text{syst.})$
2NA-QF Σ^0p	$0.54 \pm 0.20(\text{stat.})\ ^{+0.20}_{-0.16}(\text{syst.})$
2NA-FSI Σ^0p	$5.4 \pm 1.5(\text{stat.})\ ^{+1.0}_{-2.7}(\text{syst.})$
2NA-CONV Σ/Λ	$22 \pm 4(\text{stat.})\ ^{+1}_{-12}(\text{syst.})$
3NA Λpn	$1.1 \pm 0.3(\text{stat.}) \pm 0.2(\text{syst.})$
3NA Σ^0pn	$1.9 \pm 0.7(\text{stat.})\ ^{+0.8}_{-0.4}(\text{syst.})$

FINUDA at DAΦNE

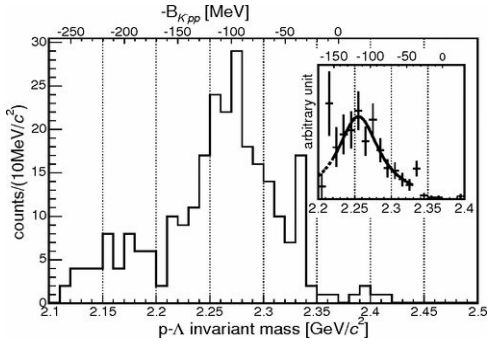

[M. Agnello et al., Phys. Rev. Lett. 94, 212303 (2005)]

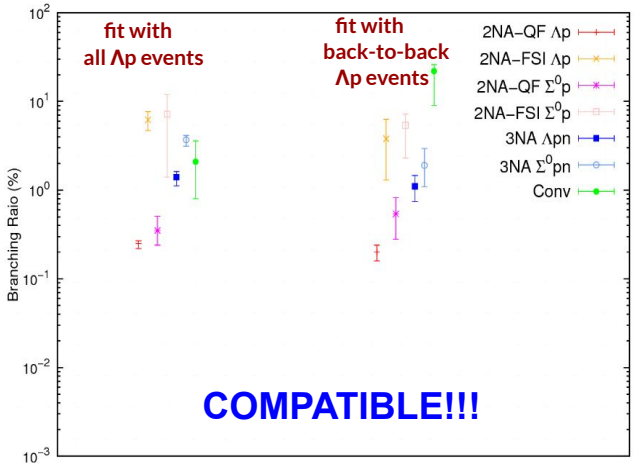

Λp analysis: K⁻ pp bound state search

R. Del Grande, K. Piscicchia, O. Vazquez Doce et al., Eur.Phys.J. C79 (2019) no.3, 190

AMADEUS at DAΦNE

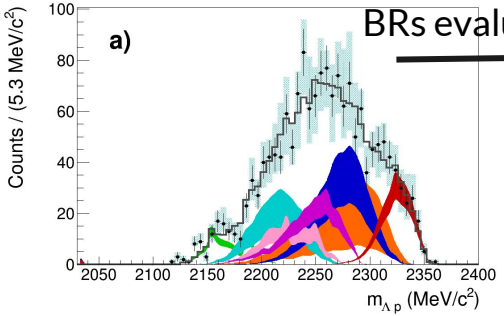

BRs evaluation

Process	Branching Ratio (%)
2NA-QF Λp	$0.20 \pm 0.04(\text{stat.}) \pm 0.02(\text{syst.})$
2NA-FSI Λp	$3.8 \pm 2.3(\text{stat.}) \pm 1.1(\text{syst.})$
2NA-QF Σ^0p	$0.54 \pm 0.20(\text{stat.})\ ^{+0.20}_{-0.16}(\text{syst.})$
2NA-FSI Σ^0p	$5.4 \pm 1.5(\text{stat.})\ ^{+1.0}_{-2.7}(\text{syst.})$
2NA-CONV Σ/Λ	$22 \pm 4(\text{stat.})\ ^{+1}_{-12}(\text{syst.})$
3NA Λpn	$1.1 \pm 0.3(\text{stat.}) \pm 0.2(\text{syst.})$
3NA Σ^0pn	$1.9 \pm 0.7(\text{stat.})\ ^{+0.8}_{-0.4}(\text{syst.})$

FINUDA at DAΦNE

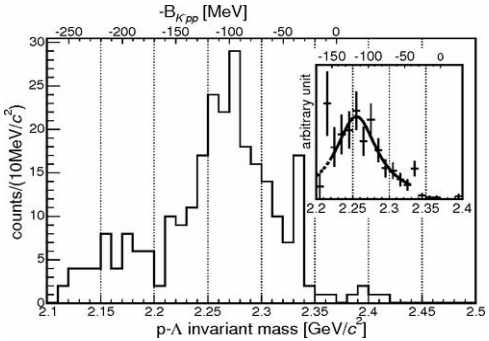

[M. Agnello et al., Phys. Rev. Lett. 94, 212303 (2005)]

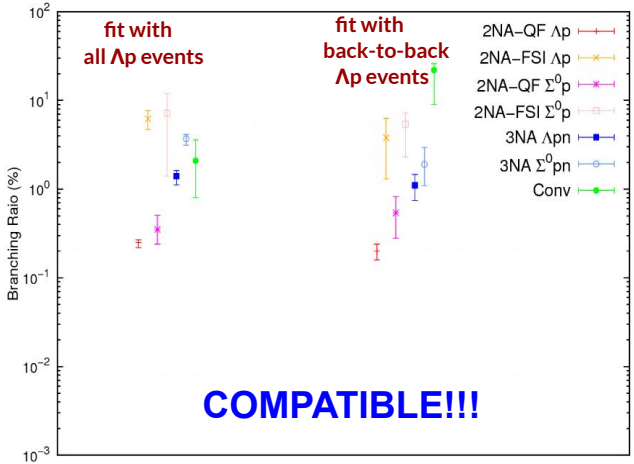

Using BE and Γ from experiments:

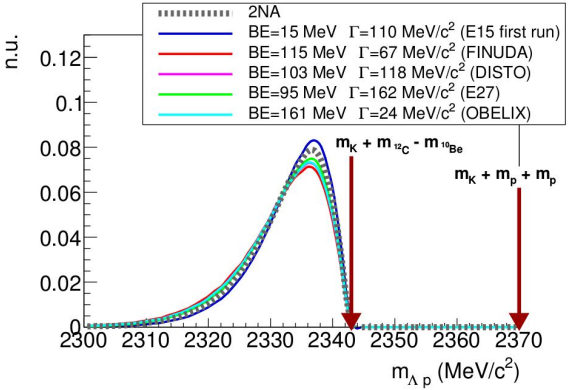

Fixing BE and moving Γ:

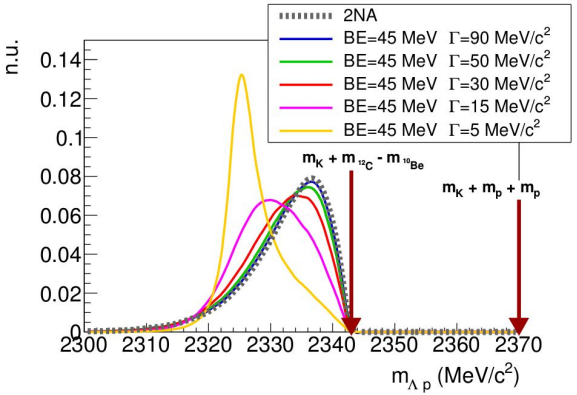

Λt analysis: Cross section and BR for 4NA

GOLDEN CHANNEL to extrapolate the K^- 4NA

$$K^- + \text{“ppnn”} \rightarrow \Lambda + t$$

Previous data:

- in ^{4}**He:** bubble chamber experiment

/M. Roosen, J. H. Wickens, Il Nuovo Cimento 66, 101 (1981)/

only **3 events** compatibile with Λt kinematics found

$$BR(K^{-4}He \rightarrow \Lambda t) = (3 \pm 2) \times 10^{-4} / K^-_{stop}$$

→ **global, no 4NA**

- in **solid targets:** ^{6,7}**Li,** ^{9}**Be** (FINUDA)

/Phys. Lett. B, 229 (2008)/

40 events, only **back-to-back data**

$$\Lambda t \text{ emission yield} \rightarrow 10^{-3} - 10^{-4} / K^-_{stop}$$

→ **global, no 4NA**

AMADEUS analysis

PRELIMINARY

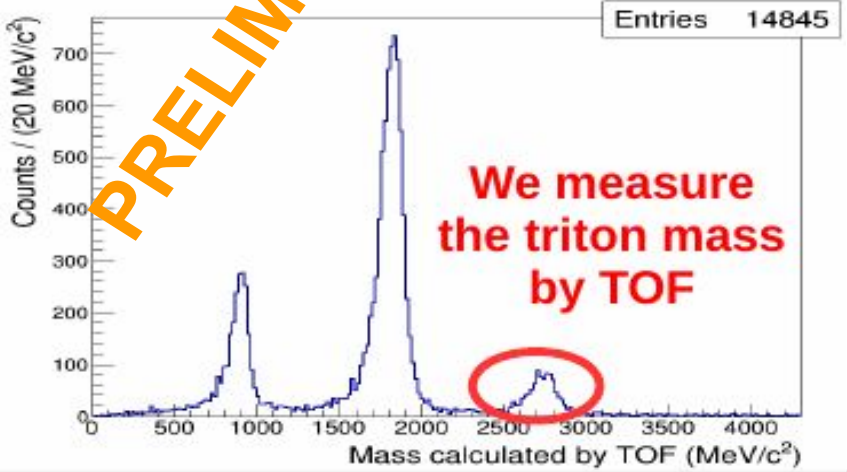

Λt analysis: Cross section and BR for 4NA in $K^- {}^4He \rightarrow \Lambda t$ process

BR($K^-{}^4He(4NA) \rightarrow \Lambda t$) **< 2.0 × 10^{-4} /K_{stop} (95% c. l.)**

σ(100 ± 19 MeV/c) ($K^-{}^4He(4NA) \rightarrow \Lambda t$) =
= (0.81 ± 0.21 (stat) $^{+0.03}_{-0.04}$ (syst)) mb

BR($K^-{}^{12}C(4NA) \rightarrow \Lambda t\ {}^8Be$) **= 1.5 ± 0.5 × 10^{-4} (stat) /K_{stop}**

σ($K^-{}^{12}C$ (4NA) $\rightarrow \Lambda t\ {}^8Be$) **= 0.58 ± 0.11 (stat) mb**

σ($K^-{}^{12}C$ (4NA) $\rightarrow \Sigma^0 t\ {}^8Be$) **= 1.88 ± 0.35 (stat) mb**

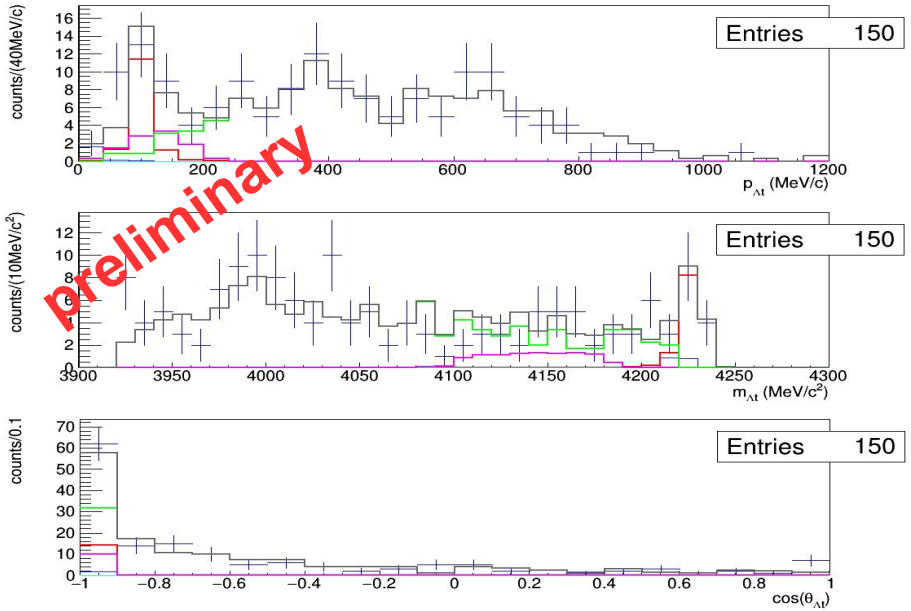

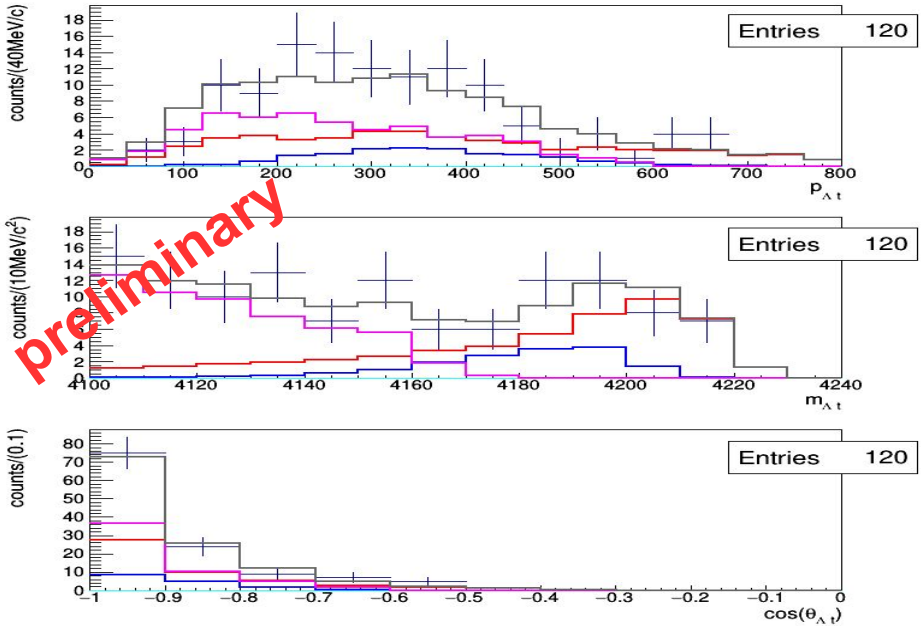

Summary

K^-n amplitude below threshold

$$|f^s_{ar}| = (0.334 \pm 0.018\,\mathrm{stat}^{+0.034}_{-0.058}\mathrm{syst})\ \mathrm{fm}\,.$$

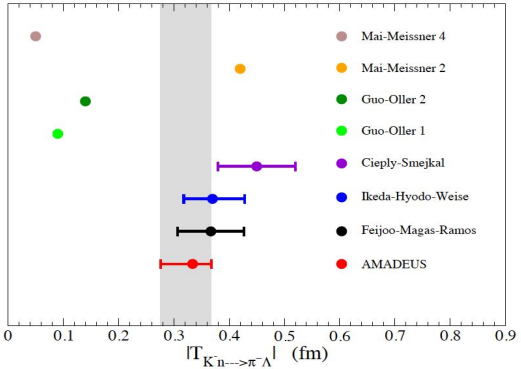

Λp channel: 2NA, 3NA and 4NA BRs and σ

Process	Branching Ratio (%)	σ (mb)	@	p_K (MeV/c)
2NA-QF Λp	0.25 ± 0.02 (stat.) $^{+0.01}_{-0.02}$(syst.)	2.8 ± 0.3 (stat.) $^{+0.1}_{-0.2}$ (syst.)	@	128 ± 29
2NA-FSI Λp	6.2 ± 1.4(stat.) $^{+0.5}_{-0.6}$(syst.)	69 ± 15 (stat.) ± 6 (syst.)	@	128 ± 29
2NA-QF Σ^0p	0.35 ± 0.09(stat.) $^{+0.13}_{-0.06}$(syst.)	3.9 ± 1.0 (stat.) $^{+1.4}_{-0.7}$ (syst.)	@	128 ± 29
2NA-FSI Σ^0p	7.2 ± 2.2(stat.) $^{+4.2}_{-5.4}$(syst.)	80 ± 25 (stat.) $^{+46}_{-60}$ (syst.)	@	128 ± 29
2NA-CONV Σ/Λ	2.1 ± 1.2(stat.) $^{+0.9}_{-0.5}$(syst.)	-		
3NA Λpn	1.4 ± 0.2(stat.) $^{+0.1}_{-0.2}$(syst.)	15 ± 2 (stat.) ± 2 (syst.)	@	117 ± 23
3NA Σ^0pn	3.7 ± 0.4(stat.) $^{+0.2}_{-0.4}$(syst.)	41 ± 4 (stat.) $^{+2}_{-5}$ (syst.)	@	117 ± 23
4NA Λpnn	0.13 ± 0.09(stat.) $^{+0.08}_{-0.07}$(syst.)	-		
Global $\Lambda(\Sigma^0)$p	21 ± 3(stat.) $^{+5}_{-6}$(syst.)	-		

$K^-p \to \Sigma^0\pi^0$ cross section

$$\sigma(K^-p \to \Sigma^0\pi^0)(p_K = (98 \pm 10) MeV/c) = 57.4 \pm 2.0(stat.)^{+3.0}_{-2.7}(syst.)\ \mathrm{mb}$$

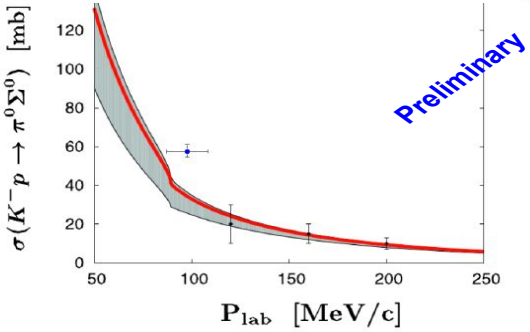

Λ t channel: 4NA BRs and σ

BR(K^{-4}He(4NA) → Λt) < 2.0×10^{-4} /K_{stop} (95% c. l.)

σ(100 ± 19 MeV/c) (K^{-4}He(4NA) →Λt) =

= (0.81 ± 0.21 (stat) $^{+0.03}_{-0.04}$ (syst)) mb

BR(K^{-12}C(4NA) → Λt ^{8}Be) = $1.5 \pm 0.5 \times 10^{-4}$ (stat) /K_{stop}

σ(K^{-12}C (4NA) →Λt ^{8}Be) = 0.58 ± 0.11 (stat) mb

σ(K^{-12}C (4NA) →Σ^0t ^{8}Be) = 1.88 ± 0.35 (stat) mb

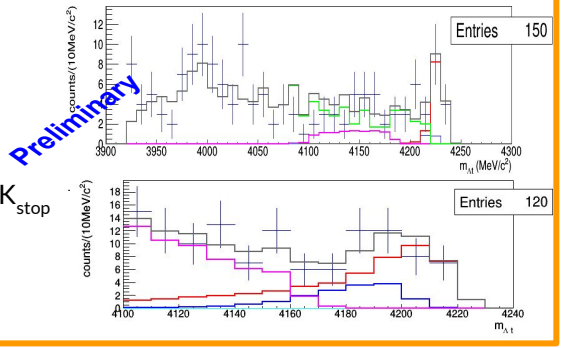

Thank You

Possible existence of kaonic bound state

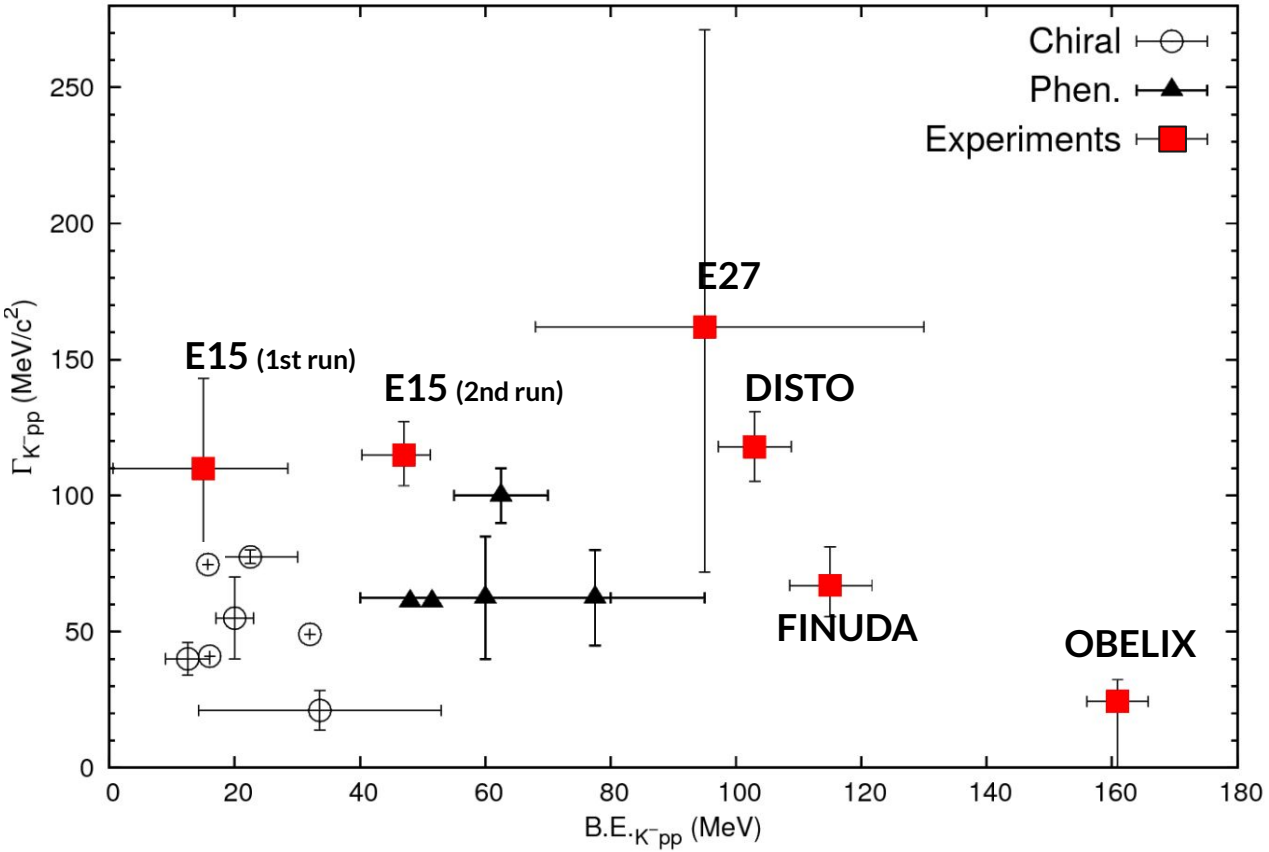

Strangeness in Neutron Stars

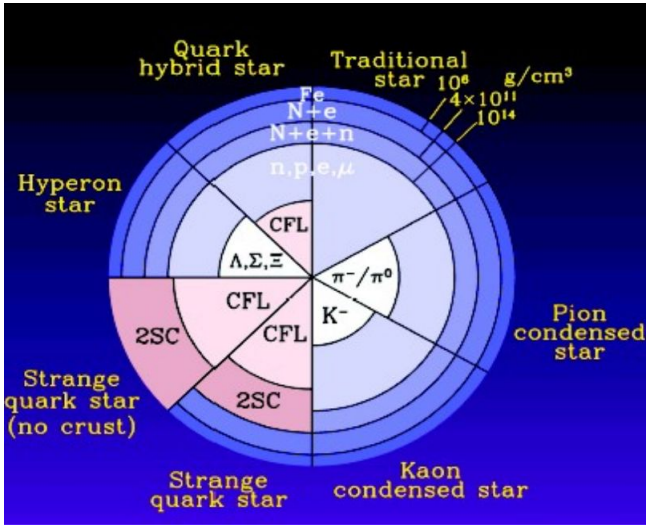

Λ-neutron matter

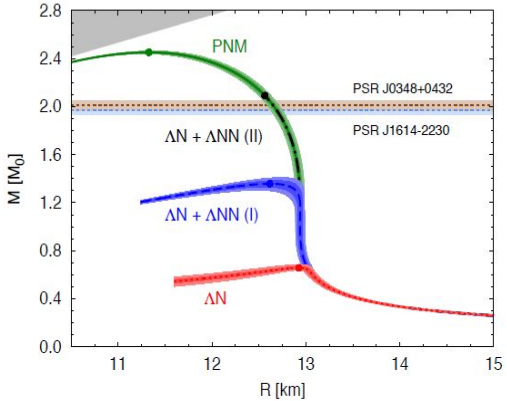

Lonardoni, Lovato, Gandolfi, Pederiva, PRL (2015)

Drastic role played by ΛNN. Calculations can be compatible with neutron star observations.

Note: no $v_{\Lambda\Lambda}$, no protons, and no other hyperons included yet...

Microscopic approach to hyperonic matter EOS

input

2BF: nucleon-nucleon (NN), nucleon-hyperon (NY), hyperon-hyperon (YY)
e.g. Nijmegen, Julich models

3BF: NNN, NNY, NYY, YYY

Hyperonic sector: experimental data

1. YN scattering (very few data)
2. Hypernuclei

Λ(1405) case

- Akaishi-Esmaili-Yamazaki phenomenological potential

Fit from $K^- + {}^4He \rightarrow \Sigma \pi {}^3H$ Bubble Chamber experiments

→ **Single pole ansatz?**

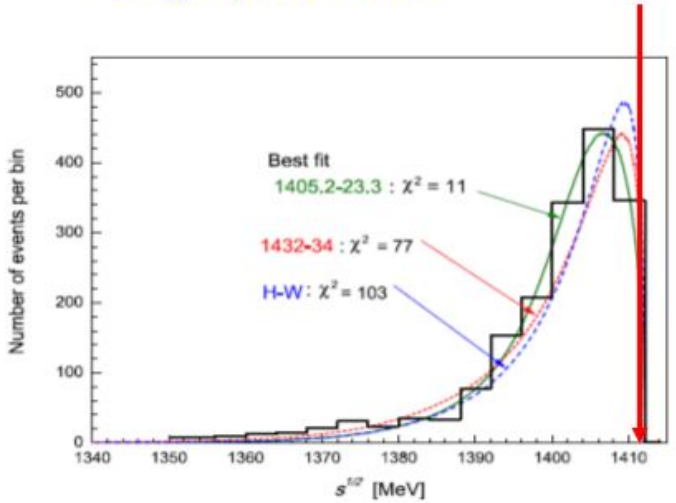

Fig. 6. Detailed differences in $M_{\Sigma\pi}$ spectra among the Hyodo–Weise prediction and the present model predictions.

[Phys. Lett. B 686 (2010) 23-28]

Two main biases:

- **the kinematical energy threshold 1412 MeV (MK + Mp - |BEp|) the high pole energy region is closed,**
- **The shape and the amplitude of the NON-RESONANT Σπ production below $\overline{K}N$ threshold is unknown.**

Resonant VS non-resonant

$K^- N \rightarrow (Y^*\ ?) \rightarrow Y \pi$

in medium, how much comes from resonance ?

Resonant VS Non-resonant

Investigated using:

$K^- \text{“n”} \rightarrow \Lambda\pi^-$ direct formation in ^4He

the goal is to measure $|f^{N\text{-}R}_{\Lambda\pi}(I=1)|$

to get information on $|f^{N\text{-}R}_{\Sigma\pi}(I=0)|$

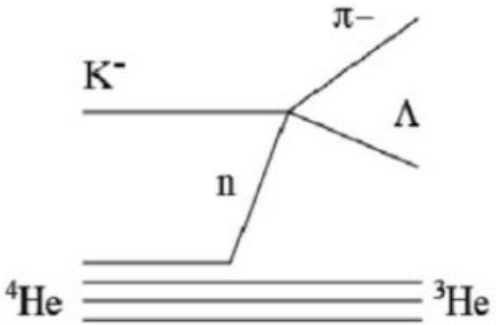

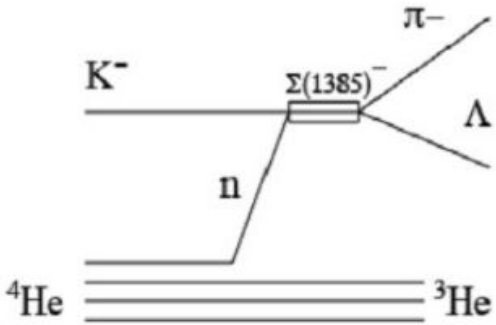

Strangeness in Neutron Stars

Hyperons are expected to appear in the core of neutron stars at $\rho \sim (2\text{-}3)\rho_0$ when μ_N is large enough to make the conversion of N into Y energetically favorable.

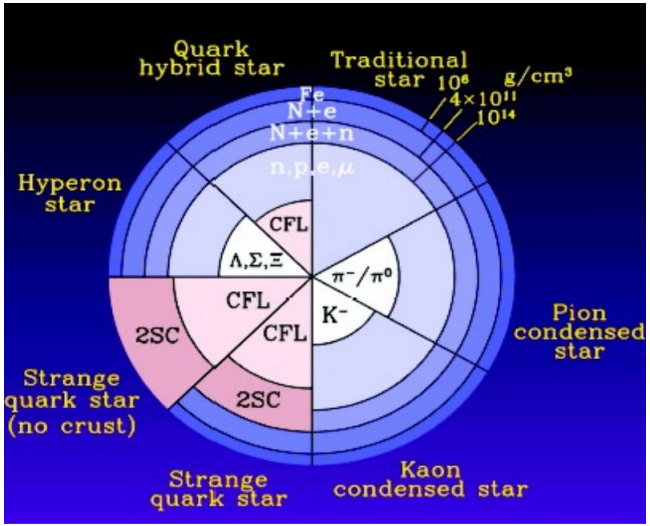

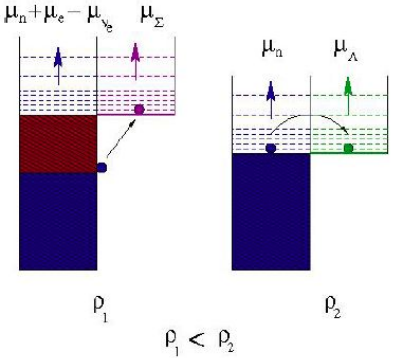

$$\mu_{\Sigma^-} = \mu_n + \mu_{e^-} - \mu_{\nu_{e^-}}$$

$$\mu_\Lambda = \mu_n$$

$$n + n \rightarrow n + \Lambda$$

$$p + e^- \rightarrow \Lambda + \nu_{e^-}$$

$$n + n \rightarrow p + \Sigma^-$$

$$n + e^- \rightarrow \Sigma^- + \nu_{e^-}$$

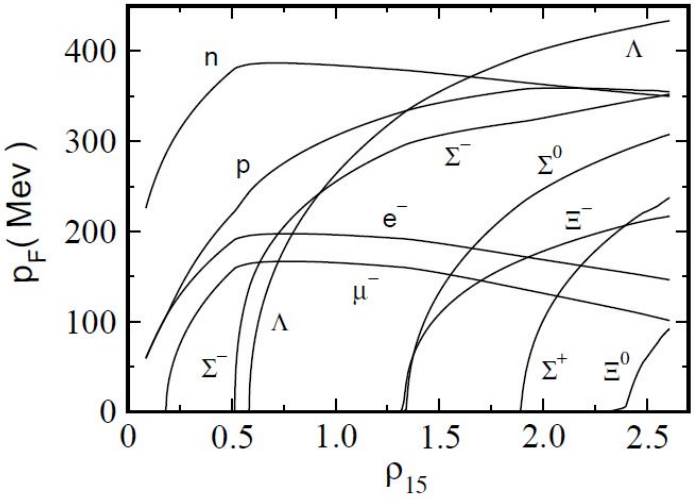

K^- absorption on light nuclei

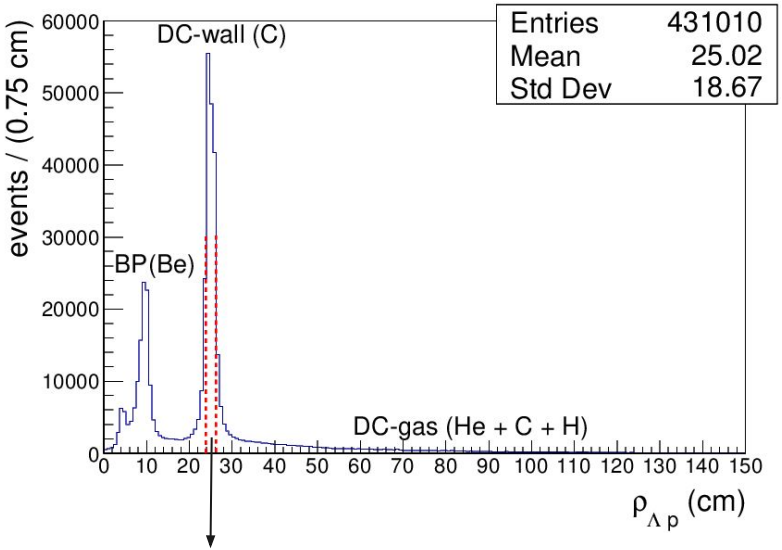

K^- absorptions in ^{12}C

$\rho_{\Lambda p} = (25.0 \pm 1.2)\ cm$

Possibility to use KLOE materials as an active target

- DC wall (750 μm C foil , 150 μm Al foil);
- DC gas (90% He, 10% C_4H_{10}).

Advantages:

Excellent resolutions..

$\sigma_{p\Lambda}$ = 0.49±0.01 MeV/c in DC gas

$\sigma_{m\gamma\gamma}$ = 18.3±0.6 MeV/c^2

Disadvantages:

Not dedicated target → different nuclei contamination → complex interpretation.